Proceedings of the ASME 2022
Fluids Engineering Division Summer Meeting
FEDSM2022
August 3-5, 2022, Toronto, Ontario, Canada

FEDSM2022-86897

CLEANING EFFECT OF BUBBLES IMPACTING TILTED WALLS UNDER ACOUSTIC WAVES

Alireza Hooshanginejad
Cornell University
Ithaca, NY

Timothy J. Sheppard
Cornell University
Ithaca, NY

Janeth Manyallah
Cornell University
Ithaca, NY

John Jaicks
Cornell University
Ithaca, NY

Sunghwan Jung
Cornell University
Ithaca, NY

ABSTRACT

The motion of bubbles near walls is ubiquitous for cleaning purposes in natural and industrial systems. Shear stress induced by bubbles on the surface is used to remove particles or bacteria adhering to the surface. In this study, we investigate the cleaning effect of bubbles on a surface coated with a protein soil solution with and without the presence of an acoustic wave transducer at a single frequency. In addition, we test different drying times for the coated surfaces before conducting the cleaning tests. Our results show that the best bubble cleaning effect occurs for the shortest drying time of the coating and an acoustic wave of 100 Hz.

Keywords: bubbles, acoustic bubbles, sustainable cleaning

NOMENCLATURE

Ω	Spin coater rotation rate
θ	Surface inclination angle
T_d	Drying time
I	Gray-scale intensity
λ	Cleaning parameter
Q	Air flow rate
$\widetilde{D}$	Averaged bubble diameter
f	Sonic wave frequency
τ	Capillary time scale
γ	Air-water surface tension
ρ	Water density

1. INTRODUCTION

Dynamics of bubbles interacting with a solid surface are widely used in many natural and industrial settings. When bubbles slide along a solid surface, they exert a shear force on the solid surface. For instance, the tickling sense that we feel from the motion of bubbles over our skin in a Jacuzzi is due to such shear forces. Such forces during the bubble impact and sliding over a surface have been theoretically studied in the past [1, 2, 3, 4]. From a practical point of view, these shear forces have been proposed as a mechanism for cleaning biological surfaces [5, 6, 7, 8, 9], or preventing biofouling growth [10]. For instance, this bubble cleaning method is proposed to sanitize soft surfaces such as fruits and vegetables without damaging fresh produce [11].

In this study, we test the effect of acoustic waves on the bubble cleaning mechanism. In addition, we examine different drying times for the coating applied on the surface. This proceeding paper is organized as follows. In Section 2 we go over different experimental methods including the coating solution preparation, the spin coating procedure, and the bubble experiments procedure. In Section 3, we present the experimental results. Finally, we discuss our results and conclude our findings in Section 4.

2. MATERIALS AND METHODS

2.1 Protein soil preparation

We first prepare a synthetic protein soil to use for coating glass slides. We first measured 100 g of 2% milk and 30 g of sifted wheat flour in a small pot. While stirring with an immersion blender, the mixture was heated to 115° C until all fluid evaporated and a paste-like solid remained. Once the mixture cooled to 30° C, it was combined with 120 g more of 2% milk. The resulting solution was stirred with an immersion blender for 10 minutes to ensure a uniform solution. 6.0 g of Nigrosin dye were then added to the mixture and gently stirred to provide a dark color to the solution for image processing purposes in cleaning experiments. The mixture was sifted twice, once through a 500-600 μm pore nylon mesh and a second time through a 100-150 μm pore stainless steel mesh.

2.2 Spin coater design

We designed a custom spin coater using Fusion 360 that was 3D printed on a desktop FDM printer (Prusa Mini+, Prusa). The base of the device was designed specifically to house and protect the Arduino Uno, potentiometer (Asin B07DHGR3ST, Twtade), and BLDC ESC motor controller (Asin B071GRSFBD, RC Electric Parts). A brushless DC drone motor (D2830, DYS) was affixed to the top of the housing and was connected to the stage. Large fin structures were modeled into the stage to minimize warping of the top surface thus preventing excessive vibration. Speed control was handled by passing the input from the potentiometer to the ESC in a pulse width modulator (PWM) signal. Two M3 screws were used to secure the glass slides to the stage prior to coating. Figure 1 shows the spin coater and its schematic. The CAD design of the spin coater parts are attached in the supplemental material

2.3 Coating procedure

On the same day as protein soils were prepared, clean glass microscope slides were coated with the protein soil solution using the spin coater, as shown in Fig. 1(b). First, we placed a clean slide on the spin coater and fastened it tightly with bolts. A 0.5 mL drop of protein soil deposited at the center of the slide was spun at a rotation rate, ω~1100-1200 rotation per minute (RPM) for 10 seconds. The coated slides were allowed to dry for 15 minutes in the lab followed by repeating the process to achieve a double coating. The slides were then stored in a cool and dry container. Variable drying times, T_d were tested in our experiments ranging from 2 to 5 days, since each slide needed at least a full day to dry.

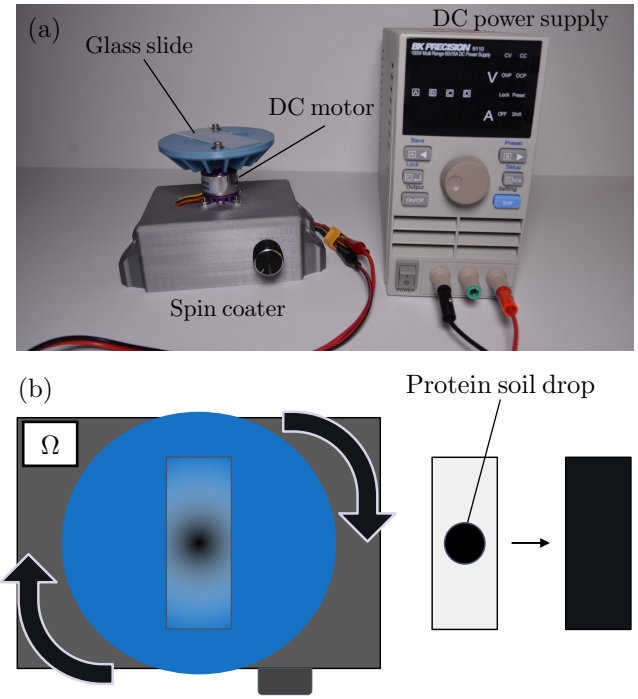

FIGURE 1: (a) A snapshot of the custom-designed spin coater that is powered by a DC power supply. (b) Slides are fastened to the center of the spin coater and are spun at ω~1100-1200 RPM for 10 seconds to allow for a thin, uniform coating across the slide.

3. RESULTS AND DISCUSSION

We filled a 20 L tank with room temperature deionized water. In this tank, we fixed a 3D printed slide holding tower that kept our microscope slides at a constant height of 11 cm and a 20-degree angle with the bottom of the tank. We then placed a 25-gauge syringe needle directly below the lowest edge of the slide holder with a fixed 5 cm distance from the slide edge. The needle generates air bubbles with an average diameter, $\bar{D}$= 0.8 mm, and a standard deviation of 0.12 mm. A 3D printed needle holder was connected through rubber tubing to a syringe and a syringe pump external to the tank. To apply acoustic waves in our experiments, we used a waterproof Bluetooth speaker (PowerAdd Co.) placed parallel to and up against the highest rising edge of the slide tower as indicated in Fig. 2(a).

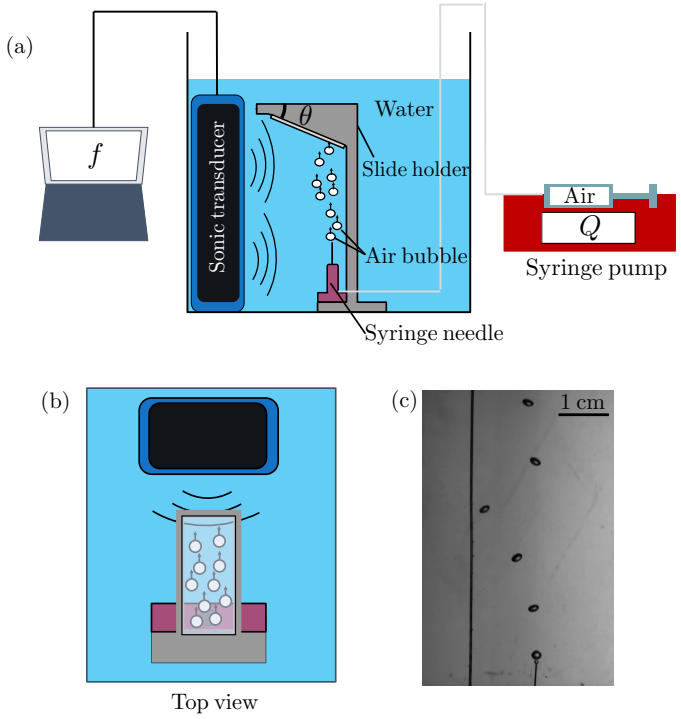

FIGURE 2: (a) Side-view schematic of the experimental setup. (b) Top view of the experimental setup. (c) A side-view snapshot of bubbles rising after pinching off from the needle. A string is used with weights at the bottom to show gravity vector direction precisely.

Slides were placed within the slide holder in the tank for 6 minutes while air is injected with a flow rate of Q=10 mL/min. During this period, air bubbles rise, impact, and slide onto the surface until they leave the surface at the higher edge. To apply acoustic waves, a sound file of a certain frequency, f, was played in the underwater speaker. This sound file was created using a custom MATLAB code. Frequency was varied between the experiments from 100 to 250 Hz.

To image our slides before and after each test, a 3D printed LED slide stand was adhered to an optical breadboard. A digital camera (Nikon 7500) was fixed 1.5 ft away from the slide stand with a 50 mm lens, a shutter speed of 1/160, an ISO of 1600, and F13 exposure. A DC power supplier continuously maintained the LED light at 3V of power. Images were taken in a dark room. The slides were imaged before and after cleaning. The slides were kept for one day to dry after the test before taking the post-test images.

To analyze the slide images, a MATLAB code was used that isolates the slide in both the pre-test and post-test images. The clean slide, pre-test and post-test images are then converted to gray-scale matrices of I_0, I_1, and I_2, respectively. We then define $\lambda = (I_2 - I_1)/(I_1 - I_0)$ as a measure of cleaning effectiveness. Hence, as λ gets closer to 1, the surface is cleaned better.

The experimental setup consists of an underwater speaker, a 20-degree 3D printed structure, and a syringe-needle combination that produces air bubbles. The speaker is set up so that the vibrations of the sound waves produced travel towards the direction of the air bubble. A single air bubble is generated from the needle using the syringe. The bubble travels up through the water before impacting a glass slide, which is glued to the 3D printed structure. A digital high-speed camera captures the air bubble's trajectory at a frame rate of 2000 fps. The video is processed in the app Tracker and the coordinates for the position of the bubble is obtained.

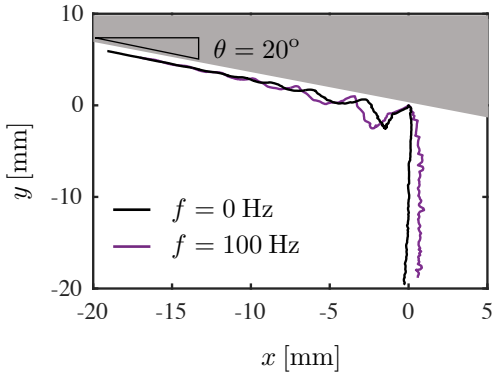

FIGURE 3: Comparison of bubble trajectory with and without acoustic waves.

Figure 3 shows the trajectory of air bubbles at 100 Hz and at 0 Hz. The acoustic waves generated by the speaker come from the left of the plot. The plots are shifted so that the first peak of the trajectory aligns. This gives us insight into the trajectory of the bubble before and after the first impact with the glass slide. We can see from the graph that as the air bubble travels up before impact, the bubble at 100 Hz was shifted to the right from the acoustic waves. There were also some left and right motions while the bubble in the non-acoustic case followed a straighter path. Additionally, in the acoustic case, the air bubble continues to bounce long after impact with the glass slide, with an increased bouncing distance and duration.

As bubbles impact and rise along the solid surface, they exert shear stress on the surface. This applied shear stress leads to the delamination of coated materials, which is the core of cleaning processes. Here, we present the results from two types of experiments: the drying time of the coating and the frequency of acoustic waves.

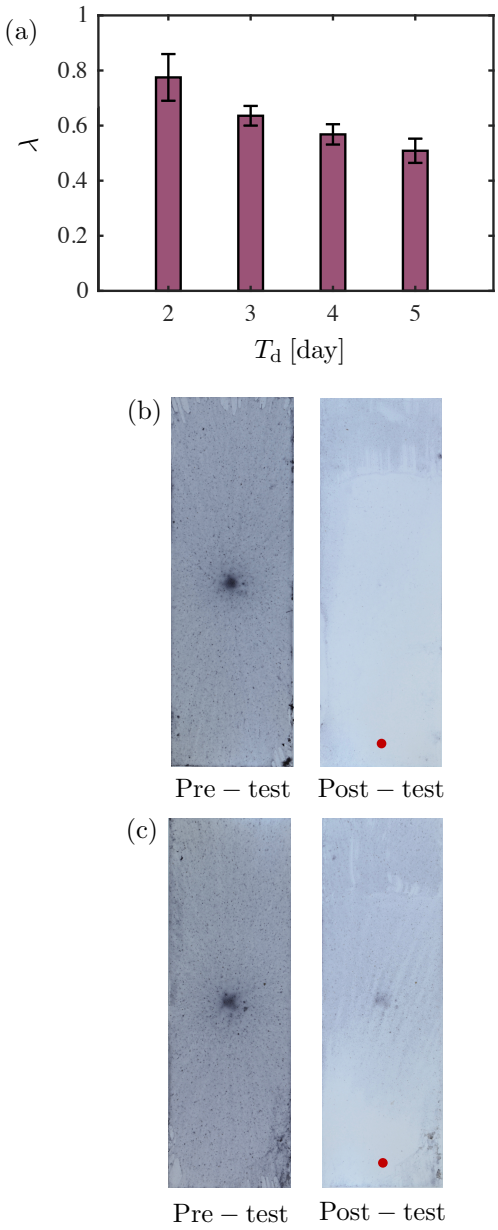

FIGURE 4: (a) The cleaning parameter, λ, for varying T_d. (b) Pretest and post-test images for T_d=3 days. (c) Pre-test and post-test images for T_d=5 days at f=100 Hz. Red dots show the projected location of the needle.

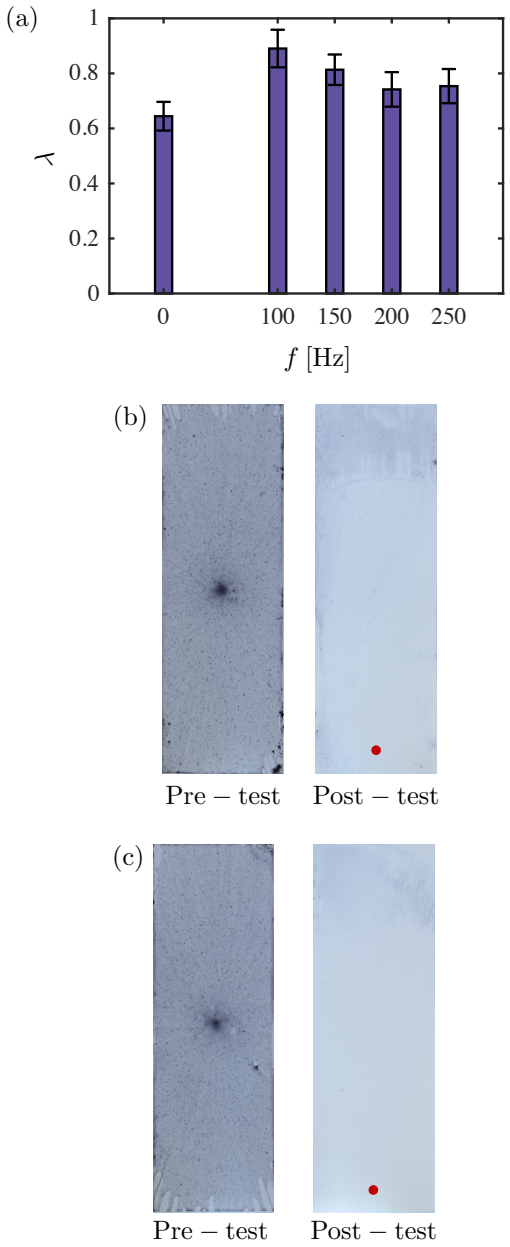

FIGURE 5: (a) The cleaning parameter, λ, for varying *f*. (b) Pretest and post-test images for *f*=0 Hz. (c) Pre-test and post-test images for *f*=100 Hz. Red dots show the projected location of the needle.

First, we tested different drying times, T_d, before conducting cleaning experiments. After the coating process, we wait at least 2 days to ensure that the coating is completely dry. We then test the coated slides in consecutive days from the second day (i.e. day 2 to day 5) to ensure that the coating condition is fixed except for the drying time. Figure 4(a) shows the cleaning parameter, λ, for different T_d. Each bar represents data points from at least three experimental trials. As indicated in Fig. 4(a), bubbles are more effective in terms of cleaning with less drying time. For instance, Fig. 4(b) shows the pre-test and post-test images of the 3-day-old surface, while Fig. 4(c) shows the corresponding images of the 5-day-long surface. The red dot in the post-test images indicated the location of the syringe needle. This decreased cleaning result with an increase in drying time is presumably due to an increase in the shear modulus and adhesion force of the coating.

Next, we investigate the effect of acoustic waves on bubble-cleaning. We apply different frequencies, *f*, ranging from 100 Hz to 250 Hz. Figure 5 shows the cleaning parameter, λ, for different *f* with θ=20° and T_d=3 days. As shown in Fig. 5(a), λ is highest at *f*=100 Hz and monotonically decreases with increasing *f*, and reaches out to a plateau to approximately λ≈0.75. Hence, using acoustic waves is not effective for frequencies larger than 150 Hz. Considering Laplace pressure in a bubble, a balance between inertia and the force of surface tension force gives rise to $\rho\bar{D}/\tau^2 \sim \gamma/\bar{D}^2$. Here, ρ denotes the water density, γ denotes the water-air surface tension, and τ denotes the characteristic time scale. This force balance leads to the characteristic time scale as $\tau \sim (\rho\bar{D}^3/\gamma)^{1/2}$. For the current range of experimental parameters, $\tau^{-1} \sim 130$ Hz. We anticipate that the cleaning effect is maximized when the external acoustic wave resonates with the bubbles at its own characteristic frequency. As shown in Fig. 5(a), the higher cleaning effects are observed between 100-150 Hz of acoustic waves. At these frequencies, the shear stress exerted on the surface increases as the bubble resonates and slides along the surface.

4. CONCLUSION

In this study, we used air bubbles to clean surfaces coated with a solution of protein soil. We used image processing tools to characterize the cleaning effects of air bubbles when the drying time of the coating varies and when the frequency of acoustic waves changes. Our results indicate that cleaning is more effective when the drying time is shorter. In addition, *f*=100 Hz provides the best cleaning results under an acoustic transducer, which is close to the resonance frequency of bubbles. Further analysis of the effect of the angle of inclination in cleaning will be conducted experimentally and numerically in the future study.

ACKNOWLEDGEMENTS

The authors thank Benjamin Cooke and Ning Ting Ni for significant contributions in the spin-coater design and acoustic experiments.

This work was supported by the National Science Foundation (NSF) under Grant No. CBET-1919753.

REFERENCES

[1] Maxworthy, T., 1991, "Bubble rise under an inclined plate," Journal of Fluid Mechanics, 229, pp. 659–674.

[2] Klaseboer, E., Manica, R., Hendrix, M. H. W., Ohl, C.-D., and Chan, D. Y. C., 2014, "A force balance model for the motion, impact, and bounce of

bubbles," Physics of Fluids, 26(9), 2022/02/14, p. 092101.
[3] Manica, R., Klaseboer, E., and Chan, D. Y. C., 2015, "Force balance model for bubble rise, impact, and bounce from solid surfaces," Langmuir, 31(24), 06, pp. 6763–6772.
[4] Esmaili, E., Shukla, P., Eifert, J. D., and Jung, S., 2019, "Bubble impact on a tilted wall: Removing bacteria using bubbles," Phys. Rev. Fluids, 4, Apr, p. 043603.
[5] Gale, G. W., and Busnaina, A. A., 1995, "Removal of particulate contaminants using ultrasonics and megasonics: A review," Particulate Science and Technology, 13(3-4), 07, pp. 197–211.
[6] Cristina, G.-S., J., B. H., and van der Mei Henny C., 2001, "Analysis of bacterial detachment from substratum surfaces by the passage of air-liquid interfaces," Applied and Environmental Microbiology, 67(6), 2022/02/12, pp. 2531–2537.
[7] Sharma, P. K., Gibcus, M. J., Van Der Mei, H. C., and Busscher, H. J., 2005, "Microbubble-induced detachment of coadhering oral bacteria from salivary pellicles," European Journal of Oral Sciences, 113(4), 2022/02/12, pp. 326–332.
[8] K., S. P., J., G. M., van der Mei Henny C., and J., B. H., 2005, "Influence of fluid shear and microbubbles on bacterial detachment from a surface," Applied and Environmental Microbiology, 71(7), 2022/02/12, pp. 3668–3673.
[9] Temesgen, T., Bui, T. T., Han, M., Kim, T.-i., and Park, H., 2017, "Micro and nanobubble technologies as a new horizon for water-treatment techniques: A review," Advances in Colloid and Interface Science, 246, pp. 40–51.
[10] Menesses, M., Belden, J., Dickenson, N., and Bird, J., 2017, "Measuring a critical stress for continuous prevention of marine biofouling accumulation with aeration," Biofouling, 33(9), 10, pp. 703–711.
[11] Lee, J. J., Eifert, J. D., Jung, S., and Strawn, L. K., 2018, "Cavitation bubbles remove and inactivate listeria and salmonella on the surface of fresh roma tomatoes and cantaloupes," Frontiers in Sustainable Food Systems, 2.